Effects of Temperature and Relative Humidity on Chloride-induced SCC Behavior of Austenitic Stainless Steel Welds

Seunghyun Kim [a*], Gi-Dong Kim [a], Jeong-Min Kim [a], Chang-Young Oh [a], Sang Woo Song [a]
[a]*Joining Technology Department, Korea Institute of Materials Science, 797 Changwondae-ro, Seongsan-Gu, Gyengsangnam-do, Korea 51508*
[*]*Corresponding author: skims@kims.re.kr*

1. Introduction

As demands on the interim storage of spent nuclear fuel arise, a dry storage is considered as promising system in worldwide. Since the system will be installed in sea shore and the canister is made of austenitic stainless steel (SS), chloride-induced stress corrosion cracking (CISCC) is considered as potential degradation mechanism[1][2]. CISCC occurs when corrosive environments, residual stress and materials' susceptibility co-exist. Therefore, it is generally known that SS welds is initiation spot for the CISCC. Also, temperature, relative humidity, and chloride concentration are key parameters for the corrosive environments. Therefore, for the investigation of the CISCC characteristics in SS welds, CISCC tests using environmental chamber and U-bend shaped specimens are carried out in different temperature and relative humidity. And the results are analyzed by electron microscopy.

2. Methods and Results

2.1 Preparation of Materials

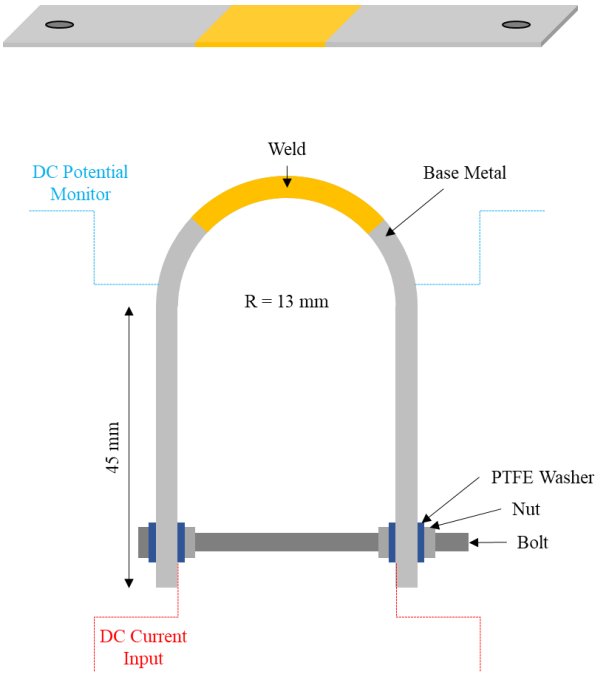

Fig. 1. Geometry of a U-bend shaped specimen.

Among commercial austenite stainless steels, 304L and 316L in size of 150 × 500 × 20(T) mm plate were prepared. Automated gas tungsten arc weld (A-GTAW) was used as welding method using Ar as a shielding gas. As welding rods, 308L and 316L were used for 304L and 316L, respectively. The weld was composed of 24 passes and prior to weld each pass, the temperature was kept under 175 °C. Weld current and voltage were set to 250 A and 15 V, respectively. The weld speed was 80 mm/min. After the welding process, corrosion test samples were fabricated in the size of 20 × 20 × 3(T) mm^3. After the process, the specimens were fabricated into a U-bend as shown in Fig. 1. For the monitoring of CISCC initiation signal using direct current potential drop (DCPD) method, current input and voltage monitoring wires were attached.

2.2 CISCC Tests

CISCC tests were carried out in salt-spray chamber with temperature and relative humidity controller as shown in Fig. 2. The tests were carried out in 1) T = 60 °C, RH = 30 %, 2) T = 50 °C, RH = 30 % and 3) T = 60 °C, RH = 20 % (RH = relative humidity). 3.5 wt.% NaCl solution was sprayed every 10 hrs for 30 mins. The immersion time was 12 weeks for each tests and 2 specimens were extracted every 3 weeks for post-mortem analysis.

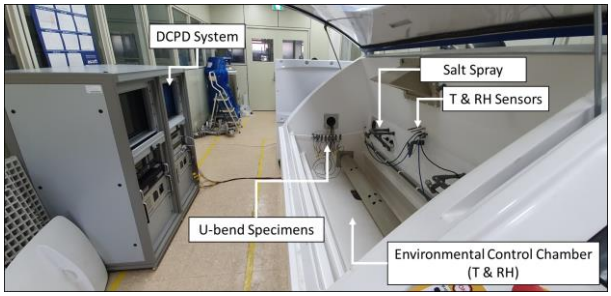

Fig. 2. Output current of the SiC detector for three particles that have been simulated as interacting in the detector randomly in time, with an average event rate of 108 events/s.

2.3 DCPD Signal Monitoring (60°C, RH 30%)

DCPD signal of the test at 60°C, RH 30% is illustrated in Fig. 3. Compared to 316L-ER316L, 304L-ER308L exhibits drastic potential increase near 800 hrs of immersion. This may indicate the evolution of crack at the pit. For the detailed analysis, the evolution of

microstructure along with immersion time will be discussed in the next section.

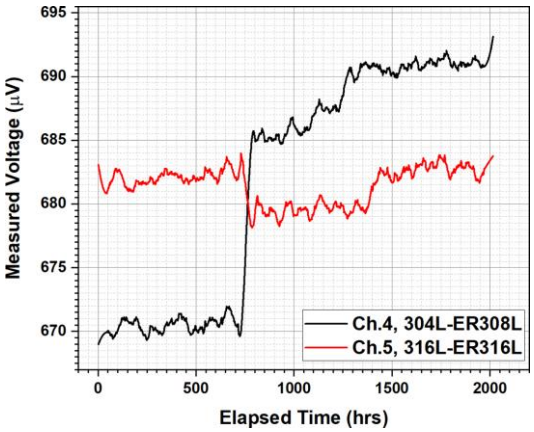

Fig. 3. DCPD monitoring results of the test at 60°C, RH 30% with material variation.

2.4 Microstructure Evolution

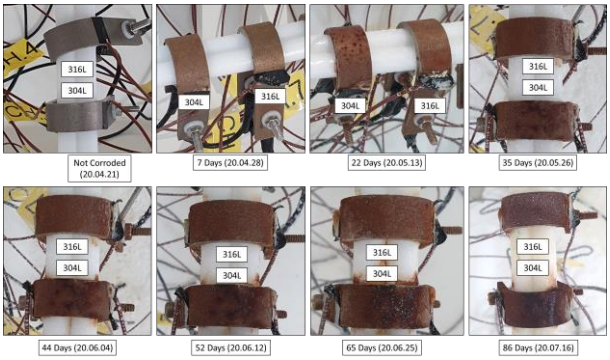

Fig. 4. Visual analysis on the evolution of the U-bend tests at 60°C, RH 30%.

Visual analysis on the evolution of the specimens of the test at 60°C, RH 30% is given in Fig. 4. As immersion time elapses, severe corrosion is found in 304L-ER308L with multiple pits. Since low Mo contents in 304L series, it is assumed that low pitting corrosion resistance results in severe pitting corrosion and moreover pit-to-crack transition in 304L-ER308L.

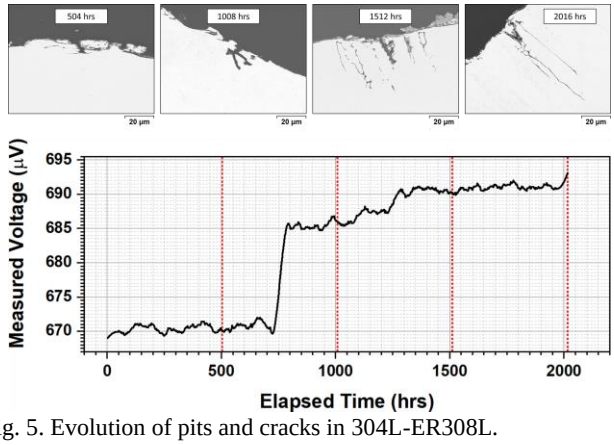

Fig. 5. Evolution of pits and cracks in 304L-ER308L.

Cross-sectional analysis on the U-bend specimens shows that there is a transition between pit and crack after 1000 hrs of immersion. The result well matches with that of DCPD signal.

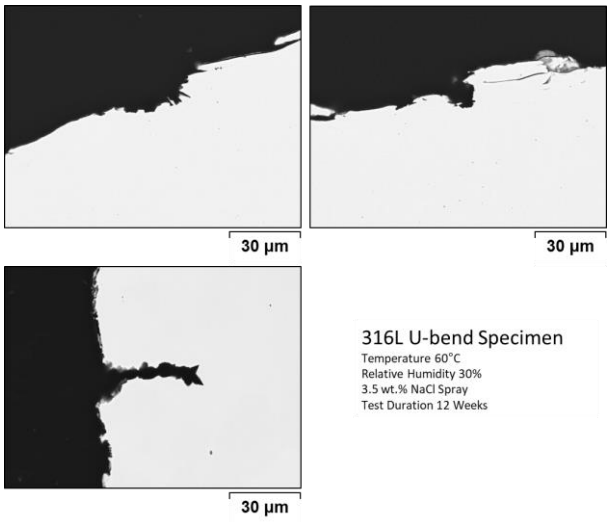

Fig. 6. Evolution of pits in 316L-ER316L

In case of 316L-ER316L, only small pits are observable in both weld and base metal. Therefore, early conjecture is that pitting corrosion resistance results in CISCC resistance in 316L compared to 304L[3]. Further analysis on the effects of types of materials, temperature, and RH will be conducted.

3. Conclusions

CISCC tests using a U-bend shaped specimens were conducted in various temperature and RH. Until now, 304L-ER308L specimens exhibits low resistance in CISCC favored environments due to pitting corrosion susceptibility. Further detailed analysis on the DCPD signals and post-mortem analysis will give the understandings on CISCC mechanism in austenitic stainless steels.

REFERENCES

[1] Y. Xie, J. Zhang, Chloride-induced stress corrosion cracking of used nuclear fuel welded stainless steel canisters: A review, J. Nucl. Mater. 466 (2015) 85–93. https://doi.org/http://dx.doi.org/10.1016/j.jnucmat.2015.07.043.

[2] L. Caseres, T.S. Mintz, Atmospheric Stress Corrosion Cracking Susceptibility of Welded and Unwelded 304, 304L and 316L Austenitic Stainless Steels Commonly Use for Dry Cask Storage Containers Exposed to Marine Engironments, 2010. http://www.nrc.gov/reading-rm/doc-collections/nuregs/contract/cr7030/.

[3] A. Schneider, D. Kuron, S. Hofmann, R. Kirchheim, AES analysis of pits and passive films formed on Fe-Cr, Fe-Mo and Fe-Cr-Mo alloys, Corros. Sci. 31

(1990) 191–196.
https://doi.org/https://doi.org/10.1016/0010-938X(90)90107-G.